

Self-supervised Video Representation Learning with Cascade Positive Retrieval

Cheng-En Wu^{1*}, Farley Lai², Yu Hen Hu¹, Asim Kadav²

¹ Department of Electrical and Computer Engineering, University of Wisconsin-Madison, WI, USA

² NEC Laboratories America, Inc., San Jose, CA, USA

{cwu356, yhhu}@wisc.edu

{farleylai, asim}@nec-labs.com

Abstract

Self-supervised video representation learning has been shown to effectively improve downstream tasks such as video retrieval and action recognition. In this paper, we present the Cascade Positive Retrieval (CPR) that successively mines positive examples w.r.t. the query for contrastive learning in a cascade of stages. Specifically, CPR exploits multiple views of a query example in different modalities, where an alternative view may help find another positive example dissimilar in the query view. We explore the effects of possible CPR configurations in ablations including the number of mining stages, the top similar example selection ratio in each stage, and progressive training with an incremental number of the final Top-k selection. The overall mining quality is measured to reflect the recall across training set classes. CPR reaches a median class mining recall of 83.3%, outperforming previous work by 5.5%. Implementation-wise, CPR is complementary to pretext tasks and can be easily applied to previous work. In the evaluation of pretraining on UCF101, CPR consistently improves existing work and even achieves state-of-the-art R@1 of 56.7% and 24.4% in video retrieval as well as 83.8% and 54.8% in action recognition on UCF101 and HMDB51. For transfer from large video dataset Kinetics400 to UCF101 and HMDB, CPR benefits existing work, showing competitive Top-1 accuracies of 85.1% and 57.4% despite pretraining at a lower resolution and frame sampling rate. The code is available at <https://github.com/necla-ml/CPR>.

1. Introduction

Recently, large-scale self-supervised pretraining such as BERT [7] and DINO [3] has been shown to improve the representations and potentially outperform its supervised counterpart. Most approaches revolve around proposing pretext

tasks [1, 9, 15, 19, 23, 37, 39, 40, 42] based on instance discrimination to learn representations by matching or classifying specific relationships between the query example and its augmented variants with the objective to minimize the contrastive loss [33] and other predictive losses. However, few address the lack of true positives (TP) other than the query example variants and likely harmful false negatives uniformly sampled from the entire dataset [6]. Previous work CoCLR [11] demonstrates the significant performance gap with the upper bound achieved in a supervised contrastive setting using the labels for TP as in [18].

We are inspired by related work [10, 13, 26, 32, 34, 36] that exploits multi-views of video to learn the representations through the correspondences between different modalities. Previous work [11, 16, 29] incorporating hard example mining in metric learning, object detection and action recognition further motivates the necessity of positive example mining in self-supervised representation learning. As for video representation learning, hard positive examples in the RGB view may be mined from the motion view despite seemingly different background appearances. On the other hand, hard positive examples in the motion view may be mined from the RGB view as the motions can differ significantly from various camera angles while the background remains similar in the RGB view for actions in the same class. CoCLR [11] shows mining in the alternative view during training improves the representations and downstream task performance. Nonetheless, it is not necessarily sufficient for mining only once in a single view to prevent sampling false positives (FP).

To address this issue, we propose the Cascade Positive Retrieval (CPR) and systematically explore as many mining configurations as possible. The idea is to refine the mining successively in a cascade of stages across different views as search with filters to be applied progressively. For instance, given a query example, one may first select those with similar background in the RGB view, then further filter out those dissimilar in the motion view and so on. Apparently, the number of mining stages and the selection ratio

*Work done as a NEC Labs intern in 2021.

in each stage matter. The goal is to conclude the strategy for effective positive example mining and make it applicable to existing work. Moreover, it remains unclear of the overall mining quality in terms of the recall across training set classes despite the R@1 mining retrieval recall by CoCLR [11]. We measure and compare the mining quality that suggests correlation with the resulting performance in ablations.

In short, we make the following contributions:

- 1.) We propose the Cascade Positive Retrieval (CPR) for self-supervised learning (SSL) of video representations that complements pretext tasks and can be applied to existing work easily regardless of the SSL framework used.
- 2.) We apply CPR to previous work and observed consistent improvement in downstream video retrieval and action recognition. We then extensively explore the design space of mining configurations in ablations w.r.t. the number of stages in the cascade, the top similar example selection ratio in each stage and the progressive training regime.
- 3.) We measure the mining quality of CPR that reaches **83.3%** recall across training set classes, outperforming the previous work by **5.5%**.
- 4.) We evaluate the transfer performance in video retrieval and action recognition on UCF101 and HMDB51 from pretraining on UCF101 and Kinetics-400 (K400) with CPR applied to an existing work. The evaluation of pretraining on UCF101 demonstrates state-of-the-art (SOTA) R@1 of **56.7%** and **24.4%** as well as accuracies of **83.8%** and **54.8%** in both downstream tasks while the transfer from K400 shows competitive accuracies of **85.1%** and **57.4%** in action recognition despite pretraining at a lower resolution and frame sampling rate.

2. Related Work

Self-supervised Learning. Large-scale representation learning through self-supervision has achieved great success in multiple fields including natural language processing (NLP) and computer vision (CV). In NLP, the general idea is to build a language model that learns to predict masked out words as in BERT [7]. In CV, the feature extraction backbone is trained to learn representations based on instance discrimination that works on both images and videos. The instance discrimination views an example and its augmented variants as positive while the other examples are treated as negative. A typical objective is to minimize the contrastive loss that encourages positive examples to be similar in representations while pushing away negative examples. Many SSL frameworks were proposed in recent

years such as SimCLR [4], BYOL [8], MoCo [5, 12] and SwAV [2] to facilitate systematic composition of numerous pretext tasks that augment the input examples and formulate the contrastive loss, delivering competitive performance in comparison with supervised counterparts. In this paper, we focus on improving self-supervised video representation learning from the perspective of hard positive example mining and show our method can be easily applied to existing work regardless of a particular SSL framework used.

Video Representation Learning. In contrast with SSL of images, videos enables rich spatiotemporal augmentation to generate diverse positive and negative example clips from sampled frames. Common pretext tasks include future prediction [10] and speed prediction [1, 15, 37, 42] to infer the relationship between clips and the pace a clip is sampled. Other tasks may require to sort out the ordering of frames or clips [40], solve jigsaw puzzles [19], match features in different modalities [13, 26, 34, 36] or group visual entities based on co-occurrences in space and time [14]. We target the video domain as videos in multiple views potentially provide opportunities to mine hard positive examples in the query class. Nonetheless, the proposed method is not limited to video tasks or specific pretext tasks. Instead, we aim to complement existing approaches with hard positive example mining.

Hard Example Mining. Hard example mining in supervised learning is well studied in metric learning and other CV tasks. In metric learning, the goal is the push away those hard negative examples but the challenge is the intractable computational overhead over large datasets as the embedding is updated constantly. One possible solution is to efficiently sample negative instances in nearest classes as in deep metric learning [29]. In video object detection, [16] leverages the temporal consistency to identify hard negative and positive examples from detection misses and isolated detection in consecutive video frames.

In the case of SSL, it is challenging for no labels and the representation learning is limited to the augmentations of the query example with instance discrimination for the lack of hard positive examples in the query class. Worse, the negative examples are uniformly sampled and potentially include false negatives (FN). This is called the sampling bias in [6] and a possible solution is to reweight the positive and negative terms in the contrastive loss for correction given the estimated class priors [6, 27].

On the other hand, as with the video object detection, self-supervised video representation learning may exploit multi-views of video clips to mine hard positive examples. CoCLR [11] mines positive examples from action recognition datasets given a query example in the RGB view with its corresponding motion or flow view. Intuitively, this may help find positive examples with similar motions de-

spite dissimilar background and vice versa. Our work further explores the possibilities to mine diverse positive examples in the query example class as CoCLR only mines positive examples in one view at a time. Chances are out of those with similar motions, top instances similar in the RGB view could be more likely the true positives. Therefore, we reshape the positive example mining as a cascade refining process between different video views. While CoCLR measures R@1 for mining retrieval recall, we further evaluate the mining quality in terms of the overall mining recall across the classes throughout training in reflection of the coverage of distinct class instances. The metric is expected to correlate with the resulting performance w.r.t. the upper bound in the supervised contrastive setting where the mining recall is essentially perfect for all the class instances being selected during training.

3. Proposed Method

Algorithm 1 CPR: Cascade Positive Retrieval

Variables: $MB, C, S, B, V, r, v_q, q_v, q, q^+$
Macros: $E(c), K(c, s), SV(s), B(e)$
Macros: $select(f_v, pos_v, r), topk(f_v, pos_v, k)$

```

1:  $C$  ▷ range of training cycles
2:  $S \leftarrow 1..n$  ▷ range of CPR stages
3:  $E(c) \in \mathbb{Z}^+$  ▷ epochs given a training cycle
4:  $K(c, s) \in \mathbb{Z}^+$  ▷ Top- $k$  to select at stage  $s$  in cycle  $c$ 
5:  $r \in \mathbb{R}^+$  ▷ selection ratio before the last stage
6:  $select(SM, r) \in \mathbb{Z}^+$  ▷ select top similar instances by ratio
7:  $topk(SM, k) \in \mathbb{Z}^+$  ▷ select by a top number  $k$ 
8:  $SV(s) \in \mathbb{Z}^+$  ▷ given a view at stage  $s$ 
9:  $V \in \{v_1, v_2, \dots\}$  ▷ set of views
10: for  $c \in C$  do
11:   for  $e \in E(c)$  do
12:     for  $(q, q^+) \in B(e)$  do
13:       for  $v \in V$  do
14:         if  $v == v_q$  then
15:            $f_{qv_q} \leftarrow encoder_{v_q}(q_{v_q})$ 
16:            $f_{q^+_{v_q}} \leftarrow encoder_{v_q}^{ema}(q^+_{v_q})$ 
17:         else
18:            $f_{q^+_{v_v}} \leftarrow encoder_v^{fixed}(q^+_{v_v})$ 
19:         end if
20:       end for
21:       for  $s \in S$  do
22:          $v \leftarrow SV(s)$ 
23:         if  $s == 1$  then
24:            $pos \leftarrow select(f_{q^+_{v_q}}, MB_v, r)$ 
25:         else if  $s == n$  then
26:            $pos \leftarrow topk(f_{q^+_{v_v}}, pos_v, K(c, s))$ 
27:            $pos = \{q^+, pos\}$ 
28:            $neg = MB \setminus pos$ 
29:         else
30:            $pos \leftarrow select(f_{q^+_{v_v}}, pos_v, r)$ 
31:         end if
32:       end for
33:        $loss \leftarrow MIL\_NCE(q_{v_q}, pos_{v_q}, neg_{v_q})$ 
34:        $optimize(encoder_{v_q}, loss)$ 
35:        $update(MB, f_{q^+_{v_q}})$ 
36:     end for
37:   end for
38: end for

```

In this section, we first revisit the concept of contrastive learning with different discrimination learning objectives.

Next, we present our CPR and in Algorithm 1, detailing the cascade positive retrieval for mining examples in general.

3.1. Instance Discrimination

Self-supervised video representation learning based instance discrimination where each instance serves as its own class has been shown effective with the contrastive loss of InfoNCE [33]. Specifically, given a set of videos V , a video clip v_i is a number of frames sampled from a video in V and its positive variant v_i^+ that can be an augmentation or another clip sampled from the same video, forming a positive pair (v_i, v_i^+) . On the other hand, a set of negative examples N^- consists of those clips $v_j^-, j \neq i$. These clips are fed into a query encoder and a key encoder to obtain the visual representations. The output features of the query, its positive augmentation and negative keys are denoted by q_i, q_i^+ , and k_j^- respectively. The InfoNCE loss is defined as follows:

$$\mathcal{L}_N = -\log \frac{\exp(q_i \cdot q_i^+ / \tau)}{\exp(q_i \cdot q_i^+ / \tau) + \sum_{j=1}^N \exp(q_i \cdot k_j^- / \tau)} \quad (1)$$

where dot product is a similarity with a temperature hyperparameter τ to adjust its scale. Intuitively, InfoNCE encourages to pull positive pairs closer while pushing away negative pairs.

3.2. Multi-instance Discrimination

In the case of multiple positive pairs, Multi-Instance InfoNCE or MIL-NCE proposed in [24] is defined as follows:

$$\mathcal{L}_M = -\log \frac{\sum_{p \in P} \exp(q_i \cdot q_p^+ / \tau)}{\sum_{p \in P} \exp(q_i \cdot q_p^+ / \tau) + \sum_{j=1}^N \exp(q_i \cdot k_j^- / \tau)} \quad (2)$$

where P is a positive set containing positive augmentation of the query and other keys with the same label as the query. For example, on an action video dataset, a *fencing* positive set includes the query video's augmentation and other videos with the *fencing* label.

3.3. Cascade Positive Retrieval

In view of issues with instance discrimination including the lack of other non-augmented positives and potential false negatives, previous work CoCLR [11] has proposed to mine positive examples in an alternative view other than the query view. However, there is a possibility that CoCLR suffers from FPs with similar motion patterns from the flow view because the mining in the alternative view is only done once such that some actions with very similar motion patterns such as *Shouput* and *ThrowDiscus* may be wrongly selected and confuse the model as shown in Figure 2. Unlike CoCLR mining heavily dependent on a single view, our CPR fully exploits the advantage of multi-views to improve the mining quality. Figure 1 illustrates that in one cascade of positive retrieval, CPR alternates between the RGB and

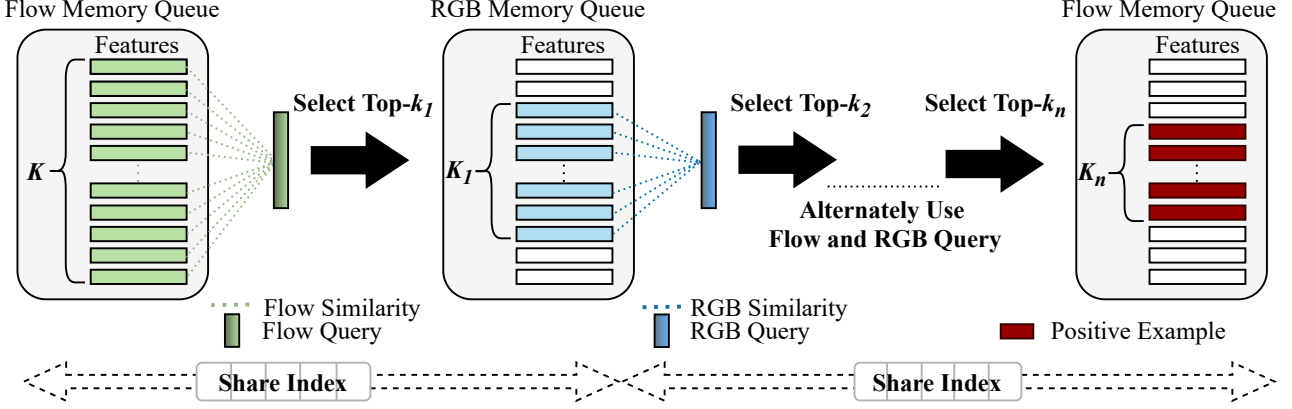


Figure 1. Overview of CPR in mining alternately from both RGB and Flow views for one cascade retrieval. K denotes the size of the memory queues storing instance features from both views. Given a query example from the RGB view, the mining starts with selecting Top- k_1 from the flow memory queue at stage 1, Top- k_2 from the RGB memory queue at stage 2, and so on up to Top- k_n from the flow memory queue at stage n . The Top- k_n instances at the final stage are selected to form the positive set.

flow views to mine a top number of positive examples with most similar appearances and motions as the query clip.

When applying CPR to existing work, there are many possible configurations and hyperparameters to consider as described in Algorithm 1 that assumes a memory bank MB storing encoded instance features in different views, a progressive training schedule in cycles, the number of epochs in one cycle, the number of mining stages in one cascade, the selection ratio of top similar examples in each stage and etc. Specifically, the algorithm iterates through each cycle c and epoch e to train with query examples in batches. Each batch consists of query examples and their positive variants from augmentation or sampling as q and q^+ . In the beginning of the batch processing, the representation encoder in the query view $encoder_{v_q}$ to train encodes the query examples q_{v_q} and produces the features $f_{q_{v_q}}$. Those q^+ may be encoded in the query view with the momentum $encoder_{v_q}^{ema}(q_{v_q}^+)$ and in the other views with frozen $encoder_v^{fixed}(q_v^+)$. Next, CPR retrieves the most similar examples in successive stages S given a selection ratio r used in stages before the last one and a Top- k for the final stage selection determined by the current cycle c and stage s . Note that the mining always uses the features of positive query variants to measure the similarities with those stored in MB by view. Eventually, a set of Top- k most likely positives are selected at the last stage as pos and combined with q^+ . The other instances in MB are viewed as negatives neg . Then the MIL-NCE loss is computed given the query examples, mined positives and negatives to optimize the encoder in the query view. Afterwards, the memory bank MB is updated with the newly encoded query example variants for the next batch training iteration. In the next section, we

will evaluate the effects of changing CPR hyperparameters in ablations as well as compare the performance with state-of-the-arts.

4. Experiments

4.1. Setup

Dataset. In this section, we conduct ablation studies and evaluation of CPR on three action recognition datasets:

HMDB51 [21] consists of 7K videos in 51 human action categories. The dataset is divided into three splits. We use the first split to conduct two downstream tasks of video retrieval and action recognition.

UCF101 [28] contains 13K videos in 101 human action classes at more diverse camera angles than HMDB51. Out of the three splits of the dataset, the first one is used for our ablations, pretraining, and downstream task evaluations.

Kinetics-400 [17] is a large-scale dataset with 240K videos in 400 action categories for us to evaluate the transfer performance of SSL with CPR. With limited resources, each video is resized to 256 pixels w.r.t. the shorter edge, cropped at a lower resolution and only sampled at 5 FPS lower than related work.

Implementations. We apply CPR to previous work IIC [31] and CoCLR [11] which already used MoCo [12]. Note that CPR is not dependent on MoCo or specific contrastive learning frameworks but for ease of demonstration. For fair comparison, we use exactly the same hyperparameters as previous work and only plug in CPR to construct the positive and negative sets for computing the MIL-NCE loss. If necessary, we even retrain previous work for the same number of epochs to compare the reproduced results. More details can be found in the supplemental materials.

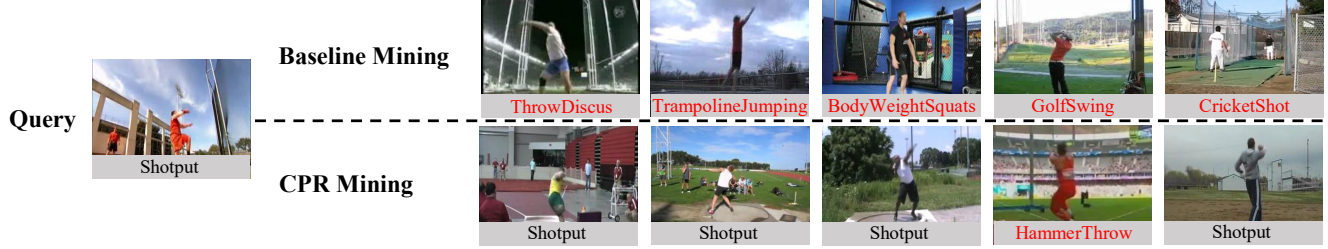


Figure 2. Qualitative Top-5 mining comparison with wrong selection in red.

Data Preprocessing: The data preparation follows previous work separately in general. As for CoCLR [11], a clip in both RGB and flow views is randomly sampled from 32 consecutive frames in the video. Each frame is randomly cropped and resized to 128×128 pixels. We apply the same data augmentations including horizontal flips, color jittering and Gaussian blur to the clips. Note that Gaussian blur is not used for downstream tasks. To generate optical flow maps from the video, we use TV-L1 [43] to extract the flow view with a third channel filled with zeros. The features are clipped in the range of 20 pixels and rescaled from $[-20, 20]$ to $[0, 255]$. In contrast, the motion view for IIC [31] is based on frame difference residuals.

Self-supervised Pretraining. For IIC [31], we train from scratch with CPR under NPID [38]. For CoCLR [11] on UCF101, we begin with the released RGB and flow models pretrained with InfoNCE as there is no positive mining in the initialization. Next at the co-training stage, the RGB and flow models are alternately trained for 400 epochs on 2 GPUs, each with a batch size of 16. That is the same number of epochs as two cycles in CoCLR. On K400, we also begin with their pretrained weights of both RGB and flow models with MIL-NCE from CoCLR as the InfoNCE checkpoints on K400 are not released yet. Then we train each model for 50 epochs and apply the same experimental settings on UCF101 except for the learning rate decayed by 1/10 at epoch 40.

Action Recognition. We evaluate the action recognition performance of the pretrained models on UCF101 and HMDB51. The pretrained models are transferred as the feature extraction backbone for downstream tasks. Two scenarios including **linear probing** and **finetuning** are considered respectively. For linear probing, we freeze the backbone while training the linear classifier only. For finetuning, we train the entire network including the backbone and the linear classifier. The training and evaluation protocols essentially follow previous work for fair comparison even with test time augmentation used.

Video Retrieval. In addition to action recognition, we also evaluate video retrieval as another downstream task on both

Stages (s)	R@1	R@5	R@10	Probe	Finetune
$s = 1$	45.1	64.0	71.9	60.0	69.5
$s = 3$	46.5	64.5	72.0	60.0	69.6
$s = 5$	47.5	65.1	73.3	60.2	70.6
$s = 7$	47.8	66.2	74.6	60.4	71.3

Table 1. Ablations with CPR applied to CoCLR w.r.t. the number of stages. CoCLR is a special case with CPR in only one stage as $s = 1$ where only the Top-5 positive candidates are selected.

SR (r)	R@1	R@5	R@10	Probe	Finetune
$r = 0.8_{(s=3)}$	46.1	63.9	72.4	60.0	69.8
$r = 0.5_{(s=3)}$	46.5	64.5	72.0	60.0	69.6
$r = 0.8_{(s=7)}$	46.2	63.6	71.7	59.6	69.9
$r = 0.5_{(s=7)}$	47.8	66.2	74.6	60.4	71.3

Table 2. Results for CPR applied to CoCLR with varied selection ratios but fixed number of stages s .

IIC(+CPR)	R@1	R@5	R@10	R@20
Baseline-Top-5	36.2	53.5	63.6	72.7
Prog-Top-1	39.4	57.5	67.6	77.2
Prog-Top-2	42.5	60.5	69.0	77.5
Prog-Top-3	44.1	62.3	70.2	77.9
Prog-Top-4	45.3	63.2	70.4	78.2
Prog-Top-5	46.2	63.6	71.4	79.2

Table 3. Improvements on video retrieval with progressive training and CPR applied to IIC [31] in 5 cycles with incremental Top- k selection. The baseline is trained with the same number of total epochs in the 5 cycles with a fixed Top- k selection in the last stage.

UCF101 and HMDB51 based on extracted features from the pretrained model without finetuning. Following the test protocol in [23, 40], we take a video in the test set as a query and use it to retrieve k -nearest neighbors in its corresponding training set. The recall at k ($R@k$) serves as the evaluation metric, which means if one of the retrieved top k nearest neighbors is from the same class as the query, it is counted as a correct retrieval result.

Settings	PMR	R@1	Finetune
$s = 1$ (CoCLR)	35.1	45.1	69.5
$s = 3, r = 0.5$	35.8	46.5	69.6
$s = 5, r = 0.5$	37.4	47.5	70.6
$s = 7, r = 0.5$	38.9	47.8	71.3

Table 4. Mean PMR, R@1 measured in the last epoch as well as fine-tuning results w.r.t. different CPR configurations.

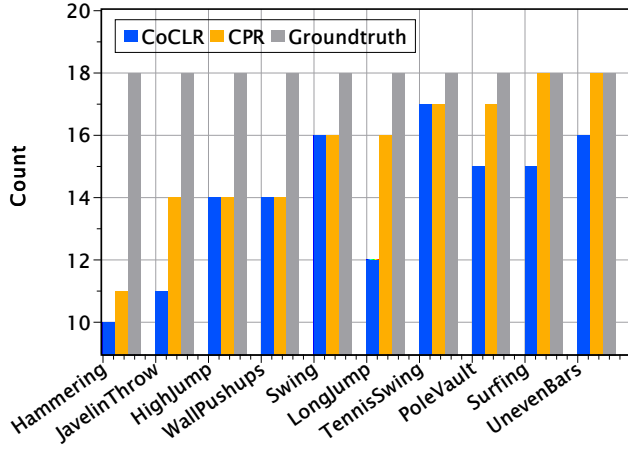


Figure 3. TP class instance mining counts in selected classes.

Method	R@1	R@5	R@10	Finetune
IIC [31]	34.8	51.6	60.8	71.8
IIC(+CPR)	46.9	63.3	71.5	73.1
CoCLR	45.1	64.1	71.9	69.5
CoCLR(+CPR)	47.8	66.2	74.6	71.3
UberNCE	70.3	81.7	86.8	80.7

Table 5. Summary of improvements over IIC and reproduced CoCLR [11] with CPR. UberNCE is reproduced in the supervised contrastive setting serving as the upper bound.

4.2. Ablation Study

In this section, we explore CPR in numerous configurations. All experiments are conducted on UCF101 following the setup mentioned in Section 4.1 except for the number of training epochs fixed at 100 for pretraining and finetuning respectively. Unless said otherwise, the ablations are based on application of CPR to CoCLR.

Number of Stages. Our CPR mines positive examples in a cascade of multiple stages. It is necessary to demonstrate the influence of this hyperparameter given a fixed selection ratio 0.5 and Top-5 for positive selection across stages before the last and the last one. As shown in Table 1, with more mining stages, the model may learn better representations for the downstream task and the best performance is

achieved in the configuration with 7 stages. As a result, we use 7 stages in later evaluation with other SOTAs.

Selection Ratio. In this ablation, we set the selection ratio (SR) to 0.5 and 0.8 respectively to evaluate the impact of SR before the final stage that is fixed to always selects Top-5. The total number of stages are set to 5 and 7 for comparison. It is observed that no matter in 5 or 7 stages, a smaller SR can get better performance in Table 2. Hence, we choose $SR = 0.5$ when comparing with other SOTAs.

Progressive Training. This configuration examines the training regime of the Top- k selection at the last stage. Specifically, is it better to train with a fixed Top- k or the training should be progressive with an incremental number of Top- k . The conclusion is likely model architecture dependent as we see the improvement with IIC shown in Table 3 in terms of video retrieval recalls but little with CoCLR. Therefore, progressive training will not be applied to CoCLR in other evaluations.

CPR Mining Quality. While CoCLR [11] measures R@1 for the mining retrieval against the ground truth (GT) throughout training, it remains unclear how many TPs are actually mined each time and throughout the training. Therefore, we measure the positive mining recall and class mining recall defined in Eq. 3 and Eq. 4:

$$\text{Positive Mining Recall} = \frac{\# TP}{\text{Size of Positive Set}} \quad (3)$$

$$\text{Class Mining Recall} = \frac{\# \text{Distinct TP Selected}}{\# \text{Total Class Instances}} \quad (4)$$

The positive mining recall (PMR) measures each time the fraction of TPs in the final Top- k selected as the positive set. The class mining recall (CMR) measures the fraction of distinct TPs selected from a class in one training epoch. Table 4 shows that as PMR and mining R@1 increase with more stages, higher fine-tuning performance on action recognition is expected. However, PMR seems to serve as a better performance indicator for being in proportion to improvement.

To further quantify the mining quality across classes, we count the number of distinct TPs selected for each action class. Figure 3 illustrates the statistics from 10 randomly chosen classes with 18 instances each in the last training epoch. CPR succeeded in selecting all the distinct TPs from both *Surfing* and *UnevenBars* classes while discovering much less from the *Hammering* class. Through visual inspection, *Hammering* is difficult with motions at different camera angles in varied scenes. In contrast, *Swing* and *Surfing* are easy to mine for having regular motion patterns and consistent background. Furthermore, we list the CMRs of the Top-3 and the bottom 3 classes respectively. The Top-3 classes are *Diving*(100%), *PommelHorse*(100%), and *UnevenBars*(100%). On the other hand, the bottom 3 classes are *Haircut*(33.3%), *Lunges*(33.3%), and *HandstandWalking*(38.8%). Out of all the UCF101 classes, CPR scores

Method	Year	Backbone	UCF101				HMDB51			
			R@1	R@5	R@10	R@20	R@1	R@5	R@10	R@20
VCOP [40]	2019	R(2+1)D	14.1	30.3	40.4	51.1	7.6	22.9	34.4	48.8
VCP [23]	2020	R3D-50	18.6	33.6	42.5	53.5	7.6	24.4	36.3	53.6
MemDPC-RGB [10]	2020	R-2D3D	20.2	40.4	52.4	64.7	7.7	25.7	40.6	57.7
MemDPC-Flow [10]	2020	R-2D3D	40.2	63.2	71.9	78.6	15.6	37.6	52.0	65.3
IIC [31]	2020	R3D-18	42.4	60.9	69.2	77.1	19.7	42.9	57.1	70.6
PacePred [37]	2020	R3D-18	23.8	38.1	46.4	56.6	9.6	26.9	41.1	56.1
CoCLR-RGB [11]	2020	S3D	53.3	69.4	76.6	82.0	23.2	43.2	53.5	65.5
CoCLR-Flow [11]	2020	S3D	51.9	68.5	75.0	80.8	23.9	47.3	58.3	69.3
DSM [34]	2021	I3D	17.4	35.2	45.3	57.8	7.6	23.3	36.5	52.5
STS [35]	2021	R3D-18	38.3	59.9	68.9	77.2	18.0	37.2	50.7	64.8
CMD [13]	2021	C3D	41.7	57.4	66.9	76.1	16.8	37.2	50.0	64.3
VCLR [20]	2021	R2D-50	46.8	61.8	70.4	79.0	17.6	38.6	51.1	67.6
MFO [25]	2021	R3D-18	39.6	57.6	69.2	78.0	18.8	39.2	51.0	63.7
MCN [22]	2021	R3D-18	53.8	70.2	78.3	83.4	24.1	46.8	59.7	74.2
CoCLR-RGB(+CPR)		S3D	50.4	66.1	73.0	80.4	18.2	40.1	52.5	66.7
CoCLR-Flow(+CPR)		S3D	56.7	75.5	82.2	88.2	24.4	48.5	62.4	74.3

Table 6. Comparison with SOTA video retrieval on UCF101 and HMDB51. Note that all methods are pretrained on UCF101.

higher CMR than baseline CoCLR in 48 classes while the baseline mines better only in 20 classes. It is even in the rest classes. Overall, CPR achieves the median CMR of **83.3%** across all the classes, which is **5.5%** improvement over the baseline CoCLR with the median CMR of 77.8%.

Besides quantitative measurements, we visualize the Top-5 positive examples mined from the baseline CoCLR and CPR for qualitative comparison. In Figure 2, the baseline mining heavily relies on the motions from optical flows and tends to select false positives (FPs) with similar motion patterns as the query. Instead, our CPR successively mines from both RGB and flow views to discover positive examples with similar appearances and motions as the query. Even the only FP still contains visually similar motions and context as the query. This indicates that CPR is able to effectively filter out potential FPs from a single view. Consequently, CPR facilitates learning representations from more diverse TPs compared with the baseline mining.

Applicability. Besides CoCLR, CPR is also applied to IIC [31] in the ablation of progressive training, demonstrating the general applicability. Particularly, IIC uses memory banks instead of momentum encoders to maintain features as well as frame difference residuals as motion views. It focuses on generating hard negatives from the query video by repeating or shuffling the frames but there is no positive example mining. With CPR, IIC gains significant performance improvements in both downstream tasks on UCF101 in Table 5 where CoCLR is also listed to show consistent performance boost. This suggests that CPR is generally applicable whether or not the existing approach has positive example mining in mind.

4.3. Comparison with State-of-the-arts

As CPR aims to benefit existing work in terms of better positive example mining, our focus is to show how much improvement an existing work can be enhanced with CPR to compete with newer SOTAs. CoCLR [11] is chosen as it already has positive example mining in mind.

Video Retrieval. To validate the effectiveness of learned representations with CPR, we evaluate the nearest neighbor video retrieval on both UCF101 and HMDB51. Specifically, the top- k video retrieval recalls for $k = 1, 5, 10, 20$ are computed as the performance metrics. As shown in Table 6, CoCLR-Flow(+CPR) outperforms the other SOTA methods in all recall metrics on both datasets. We achieve the best top-1 recall of **56.7%** on UCF101, outperforming the latest SOTA MCN [22] by 2.9% based on the same backbone. Moreover, CPR also gains much more improvement at higher top- k metrics. Since video retrieval does not require fine-tuning and leaves little room for manipulation, positive example mining from diverse positive examples across distinct videos is mostly likely the key to learning effective representations.

Action Recognition. Pretrained on UCF101, CoCLR-Flow(+CPR) outperforms all the previous SOTAs fine-tuned on UCF101 and HMDB51 with accuracies of 83.8% and 54.8% based on the same or comparable backbone and resolutions as demonstrated in Table 7.

On the other hand, due to limited resources and time, we were able to retrain with CPR the released CoCLR pretrained model that was pretrained on K400 with MIL-NCE already. Specifically, the retraining goes through the pre-training on K400 one more time with CPR and then fine-

Method	Year	Dataset	Resolution	Architecture	UCF101	HMDB51
VCOP [40]	2019	UCF101	112 × 112	R(2+1)D-26	72.4	30.9
VCP [23]	2020	UCF101	112 × 112	C3D	68.5	32.5
IIC [31]	2020	UCF101	112 × 112	R3D-18	74.4	38.3
PacePred [37]	2020	UCF101	112 × 112	R(2+1)D	75.9	35.9
PRP [42]	2020	UCF101	112 × 112	C3D	69.1	34.5
TT [15]	2020	UCF101	112 × 112	R3D-18	77.3	47.5
CoCLR-RGB [11]	2020	UCF101	128 × 128	S3D	81.4	52.1
DSM [34]	2021	UCF101	112 × 112	C3D	70.3	40.5
STS [35]	2021	UCF101	112 × 112	R3D-18	77.8	40.7
CMD [13]	2021	UCF101	112 × 112	R3D-26	76.6	47.2
MFO [25]	2021	UCF101	128 × 128	S3D	74.3	37.2
MCN [22]	2021	UCF101	128 × 128	S3D	82.9	53.8
CoCLR-RGB(+CPR)		UCF101	128 × 128	S3D	80.4	50.0
CoCLR-Flow(+CPR)		UCF101	128 × 128	S3D	83.8	54.8
MAS [36]	2019	Kinetics400	112 × 112	C3D	61.2	33.4
ST-Puzzle [19]	2019	Kinetics400	224 × 224	R3D-18	65.8	33.7
CBT [30]	2019	Kinetics400	112 × 112	S3D-G	79.5	44.6
PacePred [37]	2020	Kinetics400	112 × 112	R(2+1)D	77.1	36.6
SpeedNet [1]	2020	Kinetics400	224 × 224	S3D-G	81.1	48.8
MemDPC [10]	2020	Kinetics400	224 × 224	R2D3D	78.1	41.2
TT [15]	2020	Kinetics400	112 × 112	R3D-18	79.3	49.8
CoCLR-RGB [11]	2020	Kinetics400	128 × 128	S3D	87.9	54.6
DSM [34]	2021	Kinetics400	224 × 224	R3D-34	78.2	52.8
SeCo [41]	2021	Kinetics400	224 × 224	R2D-50	83.4	49.7
STS [35]	2021	Kinetics400	224 × 224	S3D-G	89.0	62.0
CMD [13]	2021	Kinetics400	112 × 112	R3D-26	83.7	55.2
VCLR [20]	2021	Kinetics400	224 × 224	R2D-50	85.6	54.1
MFO [25]	2021	Kinetics400	128 × 128	S3D	76.5	42.3
MCN [22]	2021	Kinetics400	128 × 128	R(2+1)D	89.2	58.8
CoCLR-RGB(+CPR)		Kinetics400	128 × 128	S3D	83.6	54.6
CoCLR-Flow(+CPR)		Kinetics400	128 × 128	S3D	85.1	<u>57.4</u>

Table 7. Comparison with SOTA action recognition on UCF101 and HMDB51 based on pretraining on UCF101 and Kinetics400.

tuning on UCF101 and HMDB51 respectively. Nonetheless, the videos in K400 are subsampled at 5FPS to save resources and the pretraining takes only 50 epochs rather than 100 with CoCLR. While the comparison is not necessarily on the same basis, CoCLR-Flow(+CPR) achieves competitive results with fine-tuning on UCF101 and HMDB51 w.r.t. other SOTAs. When compared with baseline CoCLR-RGB, CoCLR-Flow(+CPR) still improves its accuracy on HMDB51 by 2.8%. Other strong SOTAs include STS [35] trained at a much higher resolution and MCN [22] trained with meta-learning on top of self-supervised representation learning that is orthogonal to positive example mining offered by CPR.

5. Conclusion

In this work, we propose the Cascade Positive Retrieval (CPR) for self-supervised video representation learning and

extensively explored the design space of positive example mining configurations. We find that more mining stages in the cascade likely improves the performance. The positive selection ratio on the contrary works better if set to a smaller number. The progressive training with an incremental final Top- k selection could bring potential improvement. Beyond the R@1 mining retrieval recall by CoCLR [11], we further measure the mining quality quantitatively in PMR and CMR that seem to correlate with downstream task performance better. Moreover, the mining quality is also visualized for qualitative comparison. Finally, we evaluate the transfer performance from a large video dataset to smaller datasets that is either SOTA or competitive. Aside from promising results, our CPR can be applied to existing work easily regardless of SSL frameworks used. Nonetheless, the gap from the supervised contrastive performance upper bound remains, suggesting the necessity of follow-up

research for even better mining in self-supervised representation learning. In the future, we plan to facilitate the application of CPR to existing work and automate the hyperparameter search for improved mining quality.

References

- [1] Sagie Benaim, Ariel Ephrat, Oran Lang, Inbar Mosseri, William T Freeman, Michael Rubinstein, Michal Irani, and Tali Dekel. SpeedNet: Learning the speediness in videos. In *CVPR*. IEEE, June 2020. 1, 2, 8
- [2] Mathilde Caron, Ishan Misra, Julien Mairal, Priya Goyal, Piotr Bojanowski, and Armand Joulin. Unsupervised learning of visual features by contrasting cluster assignments. In *NeurIPS*, 2020. 2
- [3] Mathilde Caron, Hugo Touvron, Ishan Misra, Hervé Jégou, Julien Mairal, Piotr Bojanowski, and Armand Joulin. Emerging properties in Self-Supervised vision transformers. In *ICCV*, 2021. 1
- [4] Ting Chen, Simon Kornblith, Mohammad Norouzi, and Geoffrey Hinton. A simple framework for contrastive learning of visual representations. In *ICML*, 2020. 2
- [5] Xinlei Chen, Haoqi Fan, Ross Girshick, and Kaiming He. Improved baselines with momentum contrastive learning. *arXiv preprint*, 2020. 2
- [6] Ching-Yao Chuang, Joshua Robinson, Lin Yen-Chen, Antonio Torralba, and Stefanie Jegelka. Debaised contrastive learning. In *NeurIPS*, 2020. 1, 2
- [7] Jacob Devlin, Ming-Wei Chang, Kenton Lee, and Kristina Toutanova. BERT: Pre-training of deep bidirectional transformers for language understanding. In *ACL*, 2019. 1, 2
- [8] Jean-Bastien Grill, Florian Strub, Florent Altché, Corentin Tallec, Pierre H Richemond, Elena Buchatskaya, Carl Doersch, Bernardo Avila Pires, Zhaohan Daniel Guo, Mohammad Gheshlaghi Azar, Bilal Piot, Koray Kavukcuoglu, Rémi Munos, and Michal Valko. Bootstrap your own latent: A new approach to self-supervised learning. In *NeurIPS*, 2020. 2
- [9] Tengda Han, Weidi Xie, and Andrew Zisserman. Video representation learning by dense predictive coding. In *ICCVW*, 2019. 1
- [10] Tengda Han, Weidi Xie, and Andrew Zisserman. Memory-augmented dense predictive coding for video representation learning. In *ECCV*, Aug. 2020. 1, 2, 7, 8
- [11] Tengda Han, Weidi Xie, and Andrew Zisserman. Self-supervised co-training for video representation learning. In *NeurIPS*, Oct. 2020. 1, 2, 3, 4, 5, 6, 7, 8, 11
- [12] Kaiming He, Haoqi Fan, Yuxin Wu, Saining Xie, and Ross Girshick. Momentum contrast for unsupervised visual representation learning. In *CVPR*, Nov. 2019. 2, 4, 11
- [13] Lianghua Huang, Yu Liu, Bin Wang, Pan Pan, Yinghui Xu, and Rong Jin. Self-supervised video representation learning by context and motion decoupling. In *CVPR*, Apr. 2021. 1, 2, 7, 8
- [14] P Isola, D Zoran, D Krishnan, and E H Adelson. Learning visual groups from co-occurrences in space and time. In *ICLRW*. arxiv.org, 2016. 2
- [15] Simon Jenni, Givi Meishvili, and Paolo Favaro. Video representation learning by recognizing temporal transformations. In *ECCV*, July 2020. 1, 2, 8
- [16] Souyoung Jin, Aruni RoyChowdhury, Huaizu Jiang, Ashish Singh, Aditya Prasad, Deep Chakraborty, and Erik Learned-Miller. Unsupervised hard example mining from videos for improved object detection. In *ECCV*, pages 307–324, Jan. 2018. 1, 2
- [17] Will Kay, Joao Carreira, Karen Simonyan, Brian Zhang, Chloe Hillier, Sudheendra Vijayanarasimhan, Fabio Viola, Tim Green, Trevor Back, Paul Natsev, Mustafa Suleyman, and Andrew Zisserman. The kinetics human action video dataset. *arXiv preprint*, 2017. 4
- [18] Prannay Khosla, Piotr Teterwak, Chen Wang, Aaron Sarna, Yonglong Tian, Phillip Isola, Aaron Maschinot, Ce Liu, and Dilip Krishnan. Supervised contrastive learning. In *NeurIPS*, 2020. 1
- [19] Dahun Kim, Donghyeon Cho, and In So Kweon. Self-Supervised video representation learning with Space-Time cubic puzzles. In *AAAI*, 2019. 1, 2, 8
- [20] Haoqi Kuang, Yi Zhu, Zhi Zhang, Xinyu Li, Joseph Tighe, Sören Schwaertfeger, Cyrill Stachniss, and Mu Li. Video contrastive learning with global context. In *ICCVW*, Aug. 2021. 7, 8
- [21] H Kuehne, H Jhuang, E Garrote, T Poggio, and T Serre. HMDB: A large video database for human motion recognition. In *ICCV*, pages 2556–2563, Nov. 2011. 4
- [22] Yuanze Lin, Xun Guo, and Yan Lu. Self-Supervised video representation learning with Meta-Contrastive network. In *ICCV*, Aug. 2021. 7, 8
- [23] Dezhao Luo, Chang Liu, Yu Zhou, Dongbao Yang, Can Ma, Qixiang Ye, and Weiping Wang. Video cloze procedure for Self-Supervised Spatio-Temporal learning. In *AAAI*, Jan. 2020. 1, 5, 7, 8
- [24] Antoine Miech, Jean-Baptiste Alayrac, Lucas Smaira, Ivan Laptev, Josef Sivic, and Andrew Zisserman. End-to-End learning of visual representations from uncurated instructional videos. In *CVPR*, 2020. 3
- [25] Rui Qian, Yuxi Li, Huabin Liu, John See, Shuangrui Ding, Xian Liu, Dian Li, and Weiyao Lin. Enhancing self-supervised video representation learning via multi-level feature optimization. In *ICCV*, Aug. 2021. 7, 8
- [26] Nishant Rai, Ehsan Adeli, Kuan-Hui Lee, Adrien Gaidon, and Juan Carlos Niebles. CoCon: Cooperative-Contrastive learning. In *CVPRW*, 2021. 1, 2
- [27] Joshua Robinson, Ching-Yao Chuang, Suvrit Sra, and Stefanie Jegelka. Contrastive learning with hard negative samples. In *ICLR*, 2021. 2
- [28] Khurram Soomro, Amir Roshan Zamir, and Mubarak Shah. UCF101: A dataset of 101 human actions classes from videos in the wild. *arXiv preprint*, Dec. 2012. 4
- [29] Yumin Suh, Bohyung Han, Wonsik Kim, and Kyoung Mu Lee. Stochastic class-based hard example mining for deep metric learning. In *CVPR*. IEEE, 2019. 1, 2
- [30] Chen Sun, Fabien Baradel, Kevin Murphy, and Cordelia Schmid. Learning video representations using contrastive bidirectional transformer. *arXiv preprint*, 2019. 8

- [31] Li Tao, Xueting Wang, and Toshihiko Yamasaki. Self-supervised video representation learning using inter-intra contrastive framework. In *MM*, Aug. 2020. 4, 5, 6, 7, 8
- [32] Yonglong Tian, Dilip Krishnan, and Phillip Isola. Contrastive multiview coding. In *ECCV*, 2020. 1
- [33] Aaron van den Oord, Yazhe Li, and Oriol Vinyals. Representation learning with contrastive predictive coding. *arXiv preprint*, 2018. 1, 3
- [34] Jinpeng Wang, Yuting Gao, Ke Li, Jianguo Hu, Xinyang Jiang, Xiaowei Guo, Rongrong Ji, and Xing Sun. Enhancing unsupervised video representation learning by decoupling the scene and the motion. In *AAAI*, 2021. 1, 2, 7, 8
- [35] Jiangliu Wang, Jianbo Jiao, Linchao Bao, Shengfeng He, Wei Liu, and Yun-Hui Liu. Self-supervised video representation learning by uncovering spatio-temporal statistics. *TPAMI*, 2021. 7, 8
- [36] Jiangliu Wang, Jianbo Jiao, Linchao Bao, Shengfeng He, Yunhui Liu, and Wei Liu. Self-supervised spatio-temporal representation learning for videos by predicting motion and appearance statistics. In *CVPR*, pages 4006–4015, 2019. 1, 2, 8
- [37] Jiangliu Wang, Jianbo Jiao, and Yun-Hui Liu. Self-supervised video representation learning by pace prediction. In *ECCV*, 2020. 1, 2, 7, 8
- [38] Zhirong Wu, Yuanjun Xiong, Stella X Yu, and Dahua Lin. Unsupervised feature learning via non-parametric instance discrimination. In *CVPR*, pages 3733–3742, 2018. 5
- [39] Saining Xie, Chen Sun, Jonathan Huang, Zhuowen Tu, and Kevin Murphy. Rethinking spatiotemporal feature learning: Speed-accuracy trade-offs in video classification. In *ECCV*, 2018. 1, 11
- [40] Dejing Xu, Jun Xiao, Zhou Zhao, Jian Shao, Di Xie, and Yueting Zhuang. Self-supervised spatiotemporal learning via video clip order prediction. In *CVPR*. IEEE, June 2019. 1, 2, 5, 7, 8
- [41] Ting Yao, Yiheng Zhang, Zhaofan Qiu, Yingwei Pan, and Tao Mei. SeCo: Exploring sequence supervision for unsupervised representation learning. In *AAAI*, 2021. 8
- [42] Yuan Yao, Chang Liu, Dezhao Luo, Yu Zhou, and Qixiang Ye. Video playback rate perception for Self-supervisedSpatio-Temporal representation learning. In *CVPR*, 2020. 1, 2, 8
- [43] C Zach, T Pock, and H Bischof. A duality based approach for realtime TV-L1 optical flow. In *Joint Pattern Recognition Symposium*, pages 214–223, Heidelberg, Berlin, 2007. Springer. 5

Appendices

A. Implementation Details

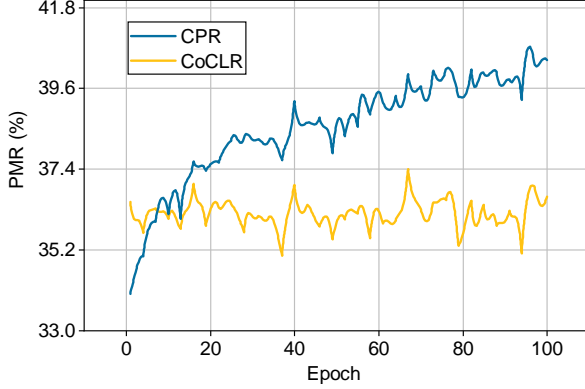


Figure 4. PMR from 1 to 100 training epochs. The results are generated by both models pretrained on UCF101.

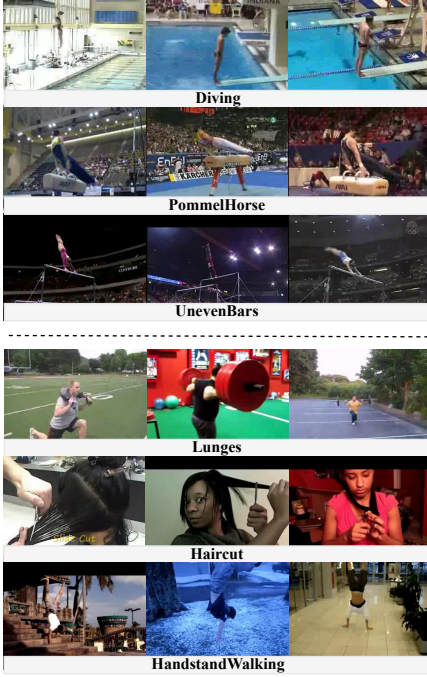


Figure 6. Visualization of the action classes that are ranked in CMR. The top half of the figure shows the Top-3 classes while the bottom of the figure shows the Bottom-3 classes.

A.1. Self-supervised Pretraining

We use MoCo [12] as the contrastive learning framework and S3D [39] as the feature extractor to implement

CPR. Note that MoCo is not required but is useful to save memory usage. Therefore, it is simply a coincidence that the baseline CoCLR [11] uses MoCo and we have applied CPR to other work not using MoCo such as IIC as well. At pretraining stage, two fully connected layers (FC1024→ReLU→FC128) are used as a projection head after the global average pooling layer to obtain the embedding features but the projection head is removed for the model to perform downstream tasks. Following CoCLR we set the momentum to 0.999, the temperature to 0.07, and the size of the queue to 2048 on every dataset except on the Kinetics-400 set to 16384. Training each model on UCF 101, we use ADAM as our optimizer with an initial learning rate of 10^{-3} and weight decay of 10^{-5} , where the learning rate is multiplied by 0.1 at 300 and 350 epochs. For kinetics-400, we apply the same experimental settings on UCF101 except for each model trained for 50 epochs and the learning rate decayed by 1/10 at epoch 40.

A.2. Action Recognition

For action recognition task, we use ADAM to optimize the model for 500 epochs with a batch size of 16 on two GPUs. The initial learning rate is set to 10^{-3} , where the learning rate is decayed by 0.1 at 400 and 450 epoch respectively. The momentum is 0.9 and the weight decay is 10^{-3} . At evaluation stage, we follow the practice of CoCLR to uniformly sample 32 frames from each video, perform ten-crop to 128×128 pixels, and then average their predictions to become the final video prediction.

B. Additional Results

B.1. Full Training PMR

In Figure 4, we provide a breakdown of full PMR during the entire pretraining process from 1 to 100 epochs on UCF101. The results show CPR gradually increases its PMR from 34.0% to 40.3%. On the other hand, PMS of baseline CoCLR is sluggish between 35.2% and 37.4%. It can be found that CPR indeed can mine more true positives by leveraging from both RGB and flow views while baseline CoCLR suffers from false positives for mining only in a single view. This is the crucial factor to support why CPR has better performance than baseline CoCLR.

B.2. Full CMR and Selective Visualizations

As shown in Figure 5, we present the full CMR in the UCF101 classes. Closer inspection of the figure reveals that CPR has the Top-3 classes are *Diving* (100%), *PommelHorse* (100%), and *UnevenBars* (100%). On the other hand, the bottom 3 classes are *Lunges* (27.8%), *Haircut* (33.3%), and *HandstandWalking* (33.3%). Furthermore, we demonstrate video frames from these classes above to visualize their content including human action and background.

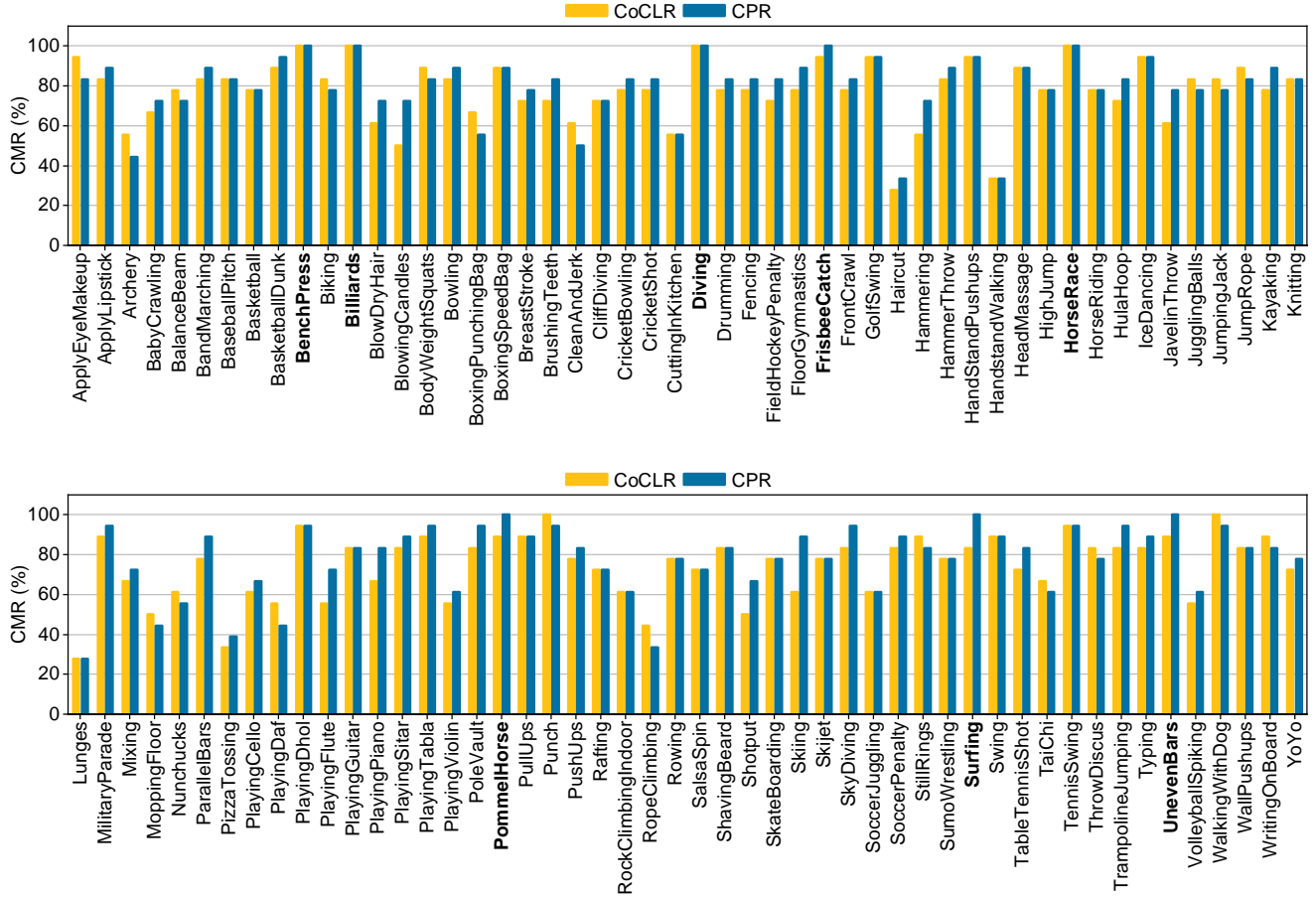


Figure 5. Class Mining Recall (CMR) per action class on UCF101. There are 101 action classes which are listed in alphabetical order. The upper bar chart covers the first 50 action classes while the lower bar chart covers the rest of the action classes. Eight action classes appeared in bold font represent cases where CPR achieves 100% CMR. They are 1. *BenchPress*, 2. *Billiards*, 3. *Diving*, 4. *HorseRace*, 5. *FrisbeeCatch*, 6. *PommelHorse*, 7. *UnevenBars*, and 8. *Surfing*. Note that we measure the CMR of both approaches in their last training epoch.

In Figure 6, sampled frames in the bottom 3 classes cover different camera angles and varied backgrounds, which increases the difficulty of mining full video instances in each class. In contrast, it is simple to discover entire video instances in each Top-3 class because these classes represent a relatively consistent background and standard motion with a fixed pattern. In the overall evaluations of all 101 classes, CPR scores higher CMR than baseline CoCLR in 48 classes while the baseline mines better only in 20 classes. It is even in the rest classes. Regarding the classes that the baseline has higher CMR, it may be that those positive classes highly correlate with a single view while CPR sometimes does not help much after visual inspection. A further comparison of the number of 100% CMR between both methods, CPR obtains eight perfect CMRs across 101 classes, which exceeds two classes compared to the baseline getting six. In addition, we evaluate the entire performance of CPR by

applying median CMR. Our approach achieves the median CMR of **83.3%** across all the classes, which outperforms the baseline with the median CMR of 77.8%. This outcome shows a great improvement with a margin of **5.5%**. In summary, these empirical evidence validates the effectiveness of our approach in mining the higher quality positives than the baseline.